Time-Dependent Numerical Simulation of Heat and Mass Transports in Water Plasma Jet with Air Entrainment

Y. Kishimoto[1] , M. Sugimoto[1] , M. Shigeta[1] , M. Tanaka[2] and T. Watanabe[2]

[1] *Department of Mechanical Systems Engineering, Tohoku University, Miyagi, Japan*
[2] *Department of Chemical Engineering, Kyushu University, Fukuoka, Japan*

Abstract: A time-dependent numerical simulation was conducted to investigate the flow dynamics of a water plasma jet ejected into air. The vortex generation at the boundary region between the water plasma jet and the ambient air was successfully captured. The ambient air was entrained into the water plasma jet by the vortices. The air entrainment caused a temperature drop near the central axis of the water plasma jet. Such an undesirable temperature decrease could deteriorate a decomposition process of substances.

Keywords: Water plasma jet, Decomposition of persistent substances, Air entrainment.

1. Introduction

Pharmaceutical and Personal Care Products, Polychlorinated Biphenyls, and Chlorofluorocarbons are water-insoluble and unburnable. Therefore, it is difficult to biodegrade or thermally decompose them. These substances are called persistent substances, and their effects on the human body and the environment are of concern.

Water plasma jets are known to be able to decompose these persistent substances, and some experimental studies and productization are carried out [1, 2]. However, the detail of the decomposition process has not yet been clarified, and it has been suggested that harmful by-products may be generated in a medium- to low-temperature range.

Nevertheless, it is difficult to obtain spatiotemporal data on flow velocity, temperature, and mole concentration for high-temperature plasma jets with temperatures ranging from several thousand to more than ten thousand K by experimental measurements. Since even numerical simulation is also arduous to reproduce vortex generation leading to heat and mass transports of a thermal plasma jet, there have been no reports for a water plasma jet. Only for an argon plasma jet, Shigeta [3] reported a similar simulation successfully capturing vortex generation and air entrainment into the plasma jet.

This study aims to clarify the dynamic behavior of the temperature and mole-concentration fields caused by air entrainment into the water plasma jet by conducting an unsteady numerical simulation using a similar method to Ref. [3].

2. Assumptions and governing equations

In this study, it is assumed that the plasma is sustained under atmospheric pressure, optically thin, and in a local thermal equilibrium state. The Coherent Structure Model [4] was applied to consider the effects of sub-grid scale (SGS) vortices, which are smaller than the grid scale (GS) vortices. The governing equations of a turbulent thermal plasma flow are the conservation equations of mass, momentum, and energy, as follows:

$$\frac{\partial \overline{\rho}}{\partial t} + \frac{\partial}{\partial x_j}\left(\overline{\rho}\widetilde{u_j}\right) = 0, \tag{1}$$

$$\frac{\partial}{\partial t}\left(\overline{\rho}\widetilde{u_i}\right) + \frac{\partial}{\partial x_j}\left(\overline{\rho}\widetilde{u_i}\widetilde{u_j}\right) + \frac{\partial \overline{p}}{\partial x_i} - \frac{\partial \overline{\tau_{ji}}}{\partial x_j} - \overline{\rho} g_i = -\frac{\partial \tau_{ji}^{\mathrm{S}}}{\partial x_j}, \tag{2}$$

$$\frac{\partial}{\partial t}\left(\overline{\rho}\tilde{h}\right) + \frac{\partial}{\partial x_j}\left(\overline{\rho}\tilde{h}\widetilde{u_j}\right) - \frac{\partial \overline{p}}{\partial t} - \widetilde{u_j}\frac{\partial \overline{p}}{\partial x_j} + \frac{\partial \overline{q_j}}{\partial x_j} - \overline{\tau_{ji}}\frac{\partial \widetilde{u_i}}{\partial x_j} + \overline{\dot{R}} = -\frac{\partial q_j^{\mathrm{S}}}{\partial x_j} + \Pi_p^{\mathrm{S}} + \varepsilon^{\mathrm{S}}, \tag{3}$$

where the superscript S represents the value at SGS, and the right-hand side of each equation shows the effect of the eddies at SGS. Here, $\overline{\phi}$ and $\tilde{\phi}$ denote the low-pass filtered and Favre filtered values of a general variable ϕ, respectively. t denotes the time. x_i is the component of the position vector. ρ, u_i, p, g_i, and h respectively stand for the density, velocity, pressure, gravitational acceleration, and enthalpy. The subscripts i and j denote directions. τ_{ji} is the shear stress due to viscosity, q_j is the thermal energy diffusion flux, and $\dot{R}$ is the radiation loss. ε^{S} and Π_p^{S} respectively related to the viscous dissipation and the effect of pressure gradient at SGS. However, Π_p^{S} is not considered in this study because it remains unclear for thermal plasma flows.

3. Numerical schemes

In the thermal plasma flow treated in this study, water plasma (an ionized gas) and ambient air (a nonionized gas) coexist while interacting with each other. Because of the large temperature difference between the two gases, thermodynamic properties and transport properties such as the density, viscosity, thermal conductivity, specific heat at constant pressure, electric conductivity, and sound speed, change significantly. The Mach number is sufficiently smaller than 1, and the flow can be considered to be incompressible in the entire region. Following the method in Ref. [3], which is able to simulate such numerically severe conditions, we discretized the convection term using a hybrid-upwind K-K (Kuwahara-Kawamura) scheme with third-order accuracy [5], the time derivative term using the Adams-Moulton method with third-order accuracy, and the diffusion and pressure gradient terms using the central differencing with second-order accuracy. The improved PISO algorithm [6] was applied to perform the numerical simulation.

The simulation was performed in the two-dimensional axisymmetric coordinate system with the origin set at the center of the plasma jet nozzle. The inner diameter of the nozzle was 1.8 mm, the volumetric flow rate was about 4.1 L/min, and the input power was 0.7 kW. The water plasma jet was injected into the air at 400 K at atmospheric pressure. The jet had a temperature and velocity distribution based on the experimental measurements [7], with the maximum temperature of 3191 K and the maximum velocity of 781.5 m/s. A staggered grid with the uniform spacing of 0.1 mm was used in the simulation with the time step width of 0.1 ms.

4. Results and discussion

Figure 1 shows a snapshot of the temperature distribution. The high-temperature jet extended downstream from the plasma jet nozzle exit. Because of the Kelvin-Helmholtz instability, vortices began to form near the boundary between the high-speed plasma jet and the ambient air from about the axial position of 20 mm. Regions where colder fluid was surrounded by hotter fluid were observed at the axial positions of 48 mm, 66 mm, and 96 mm.

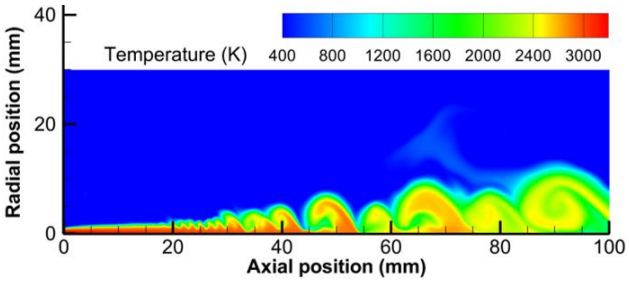

Fig. 1 Snapshot of temperature distribution.

Figure 2 shows the distribution of the mole fractions of the H_2O-derived components at the same time as Fig. 1. The vortices entrain the ambient air toward the central axis, causing the mole fraction to decrease gradually downstream in the axial direction and outward in the radial direction.

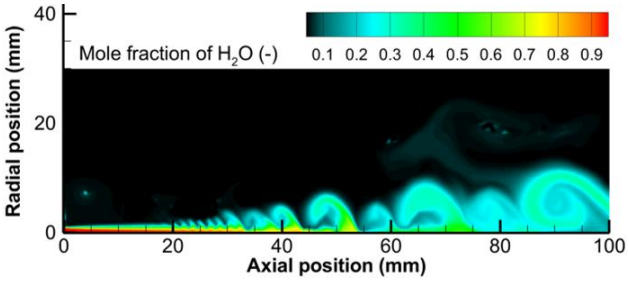

Fig. 2 Snapshot of distribution of mole fraction of H_2O.

Furthermore, the time evolutions of the mole fraction of H_2O and the temperature were investigated at two observation points on the computational domain. The two observation points were located at the axial position of 60.05 mm and the radial positions of 0.55 mm and 4.95 mm. Figure 3 shows the results of the time evolutions of the

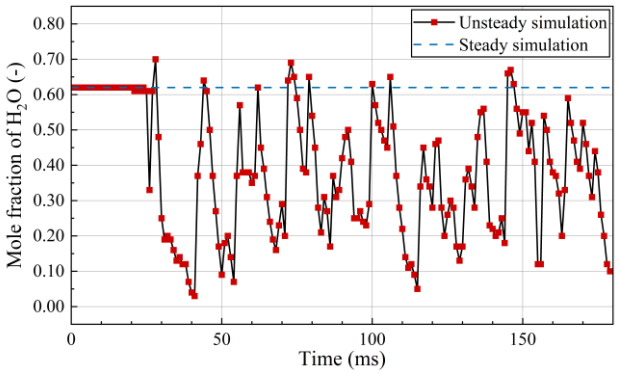

(a) At radial position of 0.55 mm.

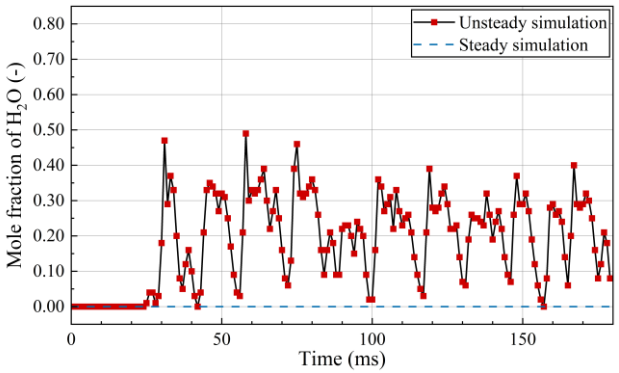

(b) At radial position of 4.95 mm.

Fig. 3 Time evolutions of mole fraction of H_2O.

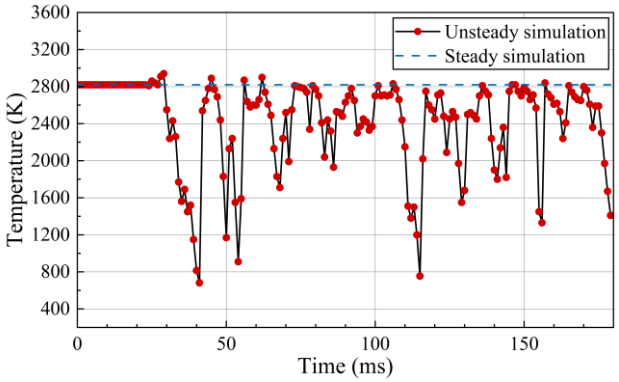

(a) At radial position of 0.55 mm.

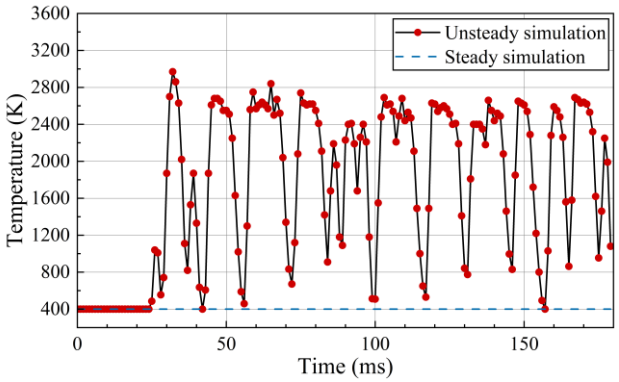

(b) At radial position of 4.95 mm.

Fig. 4 Time evolutions of temperature.

mole fraction of H_2O at each observation point during 180 ms from the start time of the unsteady simulation. Figure 3(b) shows that the mole fraction of H_2O at the outer edge of the jet was larger than that in the steady simulation. This result indicates that the components of the plasma jet are transported radially outward.

Figure 4 shows the temperature evolutions with time at the same observation points as in Fig. 3. The temperature near the central axis of the jet shown in Fig. 4(a) tended to decrease compared to the steady simulation, whereas the temperature at the outer edge of the jet shown in Fig. 4(b) tended to increase compared to the steady simulation. This indicates that the temperature in the high-temperature region near the central axis of the jet decreases due to the entrainment of the ambient air.

5. Conclusion

Time-dependent numerical simulation was performed to clarify the dynamic behavior of the temperature and mole concentration fields caused by the air entrainment into a water plasma jet. As a result, the vortex generation at the boundary region between the water plasma jet and the ambient air were successfully captured. The ambient air was entrained into the water plasma jet, and this air entrainment caused a temperature drop near the central axis of the water plasma jet. Such an undesirable temperature decrease could deteriorate a decomposition process of substances, which could lead to generation of harmful by-products.

6. References

[1] J. Heberlein and A. B. Murphy, "Thermal Plasma Waste Treatment", Journal of Physics D: Applied Physics, **41**, 5, 053001 (2008).

[2] T. Watanabe and Narengerile, "Decomposition of Glycerine by Water Plasmas at Atmospheric Pressure", Plasma Science and Technology, **15**, 4, 357 (2013).

[3] M. Shigeta, "Turbulence Modelling of Thermal Plasma Flows", Journal of Physics D: Applied Physics, **49**, 493001 (2016).

[4] H. Kobayashi, "The subgrid-scale models based on coherent structures for rotating homogeneous turbulence and turbulent channel flow", Physics of Fluids, **17**, 045104 (2005).

[5] S. Komurasaki, "A Hydrothermal Convective Flow at Extremely High Temperature", Proceeding of 7th International Conference on Computational Fluid Dynamics ICCFD7, 3001 (2012).

[6] P. J. Oliveira and R. I. Issa, "An improved PISO algorithm for the computation of buoyancy-driven flows", Numerical Heat Transfer, Part B, **40**, 473-93 (2001).

[7] A. Kanzawa and I. Kimura, "Measurements of Viscosity and Thermal Conductivity of Partially Ionized Argon Plasmas", AIAA Journal, **5**, 1315-9 (1967).